Chapter 13
Influence of Ultrasonic Waves and Airfoil-Shaped Ring Baffles on the Gas-Solid Dispersion in a CFB Riser

Vivien Rossbach, Sarah Laysa Becker, Natan Padoin, Henry França Meier, and Cintia Soares

Abstract Circulating fluidized beds (CFB) are used in several industrial applications, in which more homogeneous fluidization of solid particles is desired. In these devices, the core-annulus profile and the clusters of particles decrease the gas-solid contact. Two alternatives to improve solids dispersion are the use of aerodynamic ring-type baffles and ultrasonic waves. In this work, the influence of these devices on the solids dispersion in a lab-scale CFB riser was evaluated using Phase Doppler Anemometry (PDA) measurements. We used five airfoil-shaped ring baffles with 10 mm of thickness and 20 transducers with a frequency of 40 kHz and an input power of 10, respectively, above the riser inlet. The ring baffles increase the solid velocity near the wall and the ultrasound decreases it. With a velocity of 5.6 m/s, the solids distribution in the cross section improves with the rings and worsens with the influence of ultrasound, but with 8.3 m/s rings and ultrasound improve the solids distribution. The gas-solid dispersion improved by 18% with baffles at 8.3 m/s and 17% with ultrasound at 5.6 m/s. This study indicates that both the ring baffles and the ultrasonic field applied in the riser inlet region increase the gas-solid dispersion and contribute to reducing the concentration of particles near the riser walls and the development of clusters.

Keywords Circulating fluidized bed (CFB) · Airfoil-shaped ring baffles · Ultrasonic waves · Gas-solid dispersion

V. Rossbach · S. L. Becker · N. Padoin · C. Soares
Federal University of Santa Catarina (UFSC), Campus Universitário, s/n, Florianopolis, SC, Brazil
e-mail: natan.padoin@ufsc.br

C. Soares
e-mail: cintia.soares@ufsc.br

V. Rossbach · H. F. Meier (✉)
University of Blumenau, Rua São Paulo, Blumenau, SC 3250, Brazil
e-mail: meier@furb.br

H. F. Meier et al. (eds.), *Advances in Turbulence*, ABCM Series on Mechanical Sciences and Engineering, https://doi.org/10.1007/978-3-031-25990-6_13

13.1 Introduction

Circulating Fluidized Beds (CFB) are used in different industrial applications, as in the fluid catalytic cracking (FCC) process (Da Rosa et al. 2008), polymerization in the gaseous phase (Yan et al. 2012), ozone decomposition (Jiang et al. 1991) and oxy-coal combustion (Zhou et al. 2011). The gas-solid flow in a CFB riser is ascendant and the radial forces involved push solid particles into the riser wall, which leads to the formation of the core-annulus profile. A central dilute region with higher velocity and another region near the wall, with higher solids concentration and lower velocity, characterize this solids concentration profile (Ferschneider and Mège 2002). In processes that involve chemical reactions, as the FCC process, catalyst particles are the solids phase. Here, the first gas-solid contact occurs above the solids inlet region, and the reaction is completed rapidly. The presence of the core-annulus profile in this region decreases the contact between the catalyst particles and the gas phase containing reagents, reducing the yield of these reactions (Gan et al. 2011). In addition, a locally higher solids flux causes the particles to fall near the wall which produces back mixing and the over-cracking of products into light compounds (Namkung and Kim 1998).

Many alternatives were proposed to redistribute solid particles in the CFB riser and improve gas-solids contact in the inlet region. A viable alternative is the use of ring baffles with a variety of geometrical formats, like aerodynamic, wedged, trapezoidal, and squared baffles. These baffles are an intrusive technique that reduces the opening area and redirect solid particles from the wall to the center of a duct. Also, the use of acoustic waves is a non-intrusive way to improve gas-solids contact in the riser inlet region. Rossbach et al. (2016a, b,2019) used a set of airfoil-shaped ring-type baffles to improve solids distribution in the inlet region of a lab-scale CFB riser under dilute flow conditions. The authors studied numerically and experimentally the gas-solid flow behavior and used a statistical dispersion coefficient to evaluate the solids dispersion improvement due to the ring baffles. Four baffles with a thickness of 10 mm and an opening area of 80% were introduced below and above the solids inlet. The aerodynamic format of the baffles slows up the laminar boundary layer detachment from the surface and reduces back mixing. The solid particles were accelerated in the baffle region and redirected to the riser center. Rossbach et al. (2020) investigated the influence of ultrasonic waves on the solids dispersion in a lab-scale CFB riser. A design of experiments was conducted to find the best configuration for the ultrasonic device, including geometrical properties, sound frequency, and input power, under dilute flow conditions. As a result, the authors proposed the construction of a cylindrical device in which 20 transducers with a frequency of 40 kHz and a power of 10 W produce acoustic streaming transversally to the gas-solid flow direction. The acoustic energy increases gas turbulence and improves gas-solids mixing in the radial direction. Sufficient acoustic energy applied to the gas-solid flow can increase solids fluctuation to break up clusters of particles.

This study aims to compare the gas-solids dispersion in a lab-scale CFB riser using the ultrasonic device proposed by Rossbach et al. (2020) and the airfoil-shaped ring-type baffles of Rossbach et al. (2019). For that, experimental data of solid velocity and solid volume fraction of the two cases and the blank case were compared in the same operating conditions. We evaluated solids dispersion using the statistical dispersion coefficient proposed by Rossbach et al. (2016a) and the radial Péclet number correlation of Wei et al. (1998).

13.2 Material and Methods

This section presents the CFB experimental unit and the particle dispersion devices. The experimental methodology and the PDA technique used in the measurement of flow properties are also described.

13.2.1 Experimental Setup

The lab-scale CFB unit is presented in Fig. 1. Air at ambient conditions enters the riser base (1) when suctioned by an exhauster positioned at the riser outlet, while the solid particles are fed through the inclined duct (2), coming from a storage vessel (3), whose mass flow is controlled by a rotating valve. In this study, glass spheres with a specific mass of 2450 kg/m^3 and an average surface diameter of 80 μm were used as a solid phase. Air with solid particles exits on top of the riser, where a cyclone collects these particles and the air is directed to a bag filter. The riser outlet has an inclination of 12° relative to the solids inlet (2), as stated in Fig. 1a. the riser has a height of 2.667 m and an internal diameter of 0.104 m, as stated in Fig. 1c. The solids inlet has an internal diameter of 0.044 m, an inclination of 45° relative to the vertical line, and is positioned 40 cm above the gas inlet.

The ultrasonic device illustrated in Fig. 1b is positioned 70 cm above the gas inlet and has a total height of 0.092 m. In this device, 20 Manorshi MSO-P1640H12T transmitters with a width of 10 mm and an external diameter of 16 mm were arranged in 4 rows facing each other on the x and y axes shown in the figure. Each row has 5 transducers equally spaced for a vertical distance of 3 mm. The transducers have a frequency of 40 kHz, a sound pressure level of 115 dB, and individual electric power of 10 W. Taking into account the reference pressure of 20 μPa, it is considered that the set of transducers produces a sound pressure level of 128 dB in the internal flow to the riser. In this design, ultrasonic waves were generated on an Arduino UNO board using the code developed by Marzo et al. (2017). Square waves equivalent to sinusoidal waves with a frequency of 40 kHz are produced and delivered to an H-L298n bridge. The H-L298n bridge amplifies the power of the wave and delivers it to the transmitters, where these electrical signals are converted into acoustic signals. If the distance between two transducers arranged opposite each other is equal to

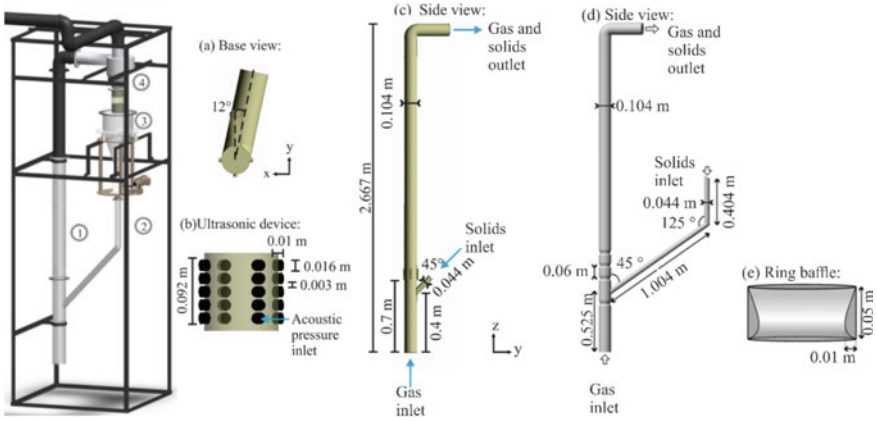

Fig. 1 Geometry of the CFB unit and the experimental devices: **a** base view of the gas and solids outlet; **b** ultrasonic device; **c** side view of the lab-scale CFB riser with the ultrasonic device; **d** side view of the riser with airfoil-shaped ring baffles; **e** geometry of the ring baffles

the internal diameter of the riser, the ratio between this distance and the half of a wavelength results in 24.04 pressure nodes that are formed. As this is not an integer value, the acoustic field produced is slightly non-resonant. However, one must also consider the acoustic field deformation caused by the gas-solid flow transversal to it and the interaction between the acoustic fields of the neighboring transducers.

The ring baffles were manufactured in polypropylene, with the geometrical properties stated in Fig. 1e. Each baffle has a height of 0.05 m and a thickness of 10 mm, resulting in an internal opening area of 80% relative to the duct area. Four baffles were inserted into the riser, the first being below the solids inlet and the others above, with 60 mm from each other, as illustrated in Fig. 1d.

Table 1 describes the operating conditions used in the experiments, both with ring baffles and acoustic waves. The ambient air velocity was varied by 5.7 m/s and 8.3 m/s and the mass flow of solids was varied by 1.60 kg/m^{2}s and 2.93 kg/m^{2}s. These operating conditions are limited by the capacity of the experimental unit and produce solid loadings compatible with the measurement technique used because the PDA technique has limitations in measuring concentrated particulate flows. In this study, we also aim to detect the formation of particle clusters in the inlet region and the core-annulus flow in the riser wall, which occur less frequently in diluted flows (Bi and Grace 1995) such as those adopted. However, these phenomena can be observed even in diluted flows, because of the instabilities generated by the collisions between particles and the high turbulence (Helland et al. 2007). Table 1 shows the solids mass loading and the solids-to-gas ratio corresponding to the 4 operating conditions studied. An analysis using the fluidization diagram of Bi and Grace (1995) shows that conditions 1 and 2 are in the limits of fast fluidization, while conditions 3 and 4 are classified as dilute phase transport. According to Bi and Grace (1995), a fast fluidization regime is characterized by a higher concentration of particles at the base

Table 1 Operating conditions of the experiments

Operating condition	v_g (m/s)	G_s (kg/m^{2}s)	Solids mass loading (kg sol./kg gas)	Solids-to-gas ratio (kg sol./m^3 gas)
1	5.7	1.60	0.23	0.28
2	5.7	2.93	0.43	0.51
3	8.3	2.93	0.29	0.35
4	8.3	1.60	0.16	0.19

and a diluted top region. The diluted phase transport regime may or may not exhibit a core-annular profile.

13.2.2 PDA Measurements

The PDA technique was used to gain experimental data from the gas-solid flow with acoustic waves, with deflector rings, and without solid dispersion devices. The error of this measurement technique is lower than 1% for the velocity and 5% for the particle diameter and concentration (Werther 1999). Dantec Dynamics A/S anemometer was used to perform non-invasive optical measurements of velocity, concentration, and diameter of the solid particles keeping the experimental design proposed in Table 2. An acquisition time of 60 s was adopted, to guarantee that over 2000 particles were measured at each point and that the time average of the measurements was the same at all points. The software BSA Flow was used to determine particle velocity from the Doppler frequency. The concentration and diameter of the particles were measured using a 112 mm PDA probe as a receiver (Rossbach et al. 2020a). The measurements were made at points along the cross section, at a height of 0.80 m from the gas inlet, as shown in Fig. 2. The measurement points were used to plot solid velocity and solid volume fraction profiles on the x and y axes. Mean data was also transformed using polar coordinates to get maps of properties in the cross section.

Table 2 PDA configurations for the experimental measurements of the gas-solid flow in the CFB riser

Acquisition time	60 s
Scattering angle	50°
Focal distance to the transmitter	300 mm
Focal distance to the receptor	310 mm
Polarization direction	Negative
Scattering mode	1st order refraction
Phase-validation ratio	30%
Refraction index	1.51
Laser power	70 mW

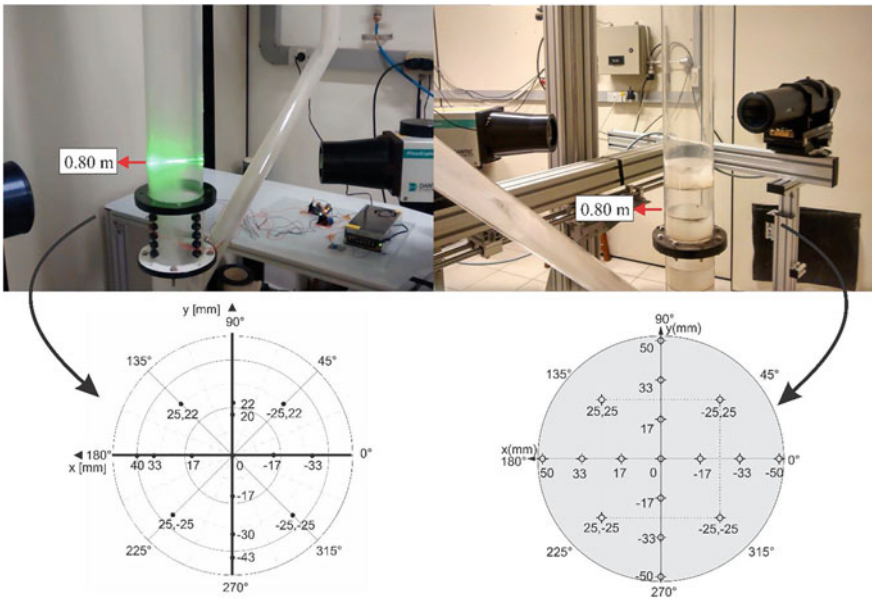

Fig. 2 Illustration of the experimental setup and maps of points measured in the cross section of the riser at 0.80 m height

13.2.3 Solids Dispersion Coefficient

Solids dispersion along the cross section of the riser at a height of 0.80 m was evaluated using the statistical dispersion coefficient as proposed by Rossbach et al. (2019). Gas-solid dispersion was also evaluated, using the correlation for the radial Péclet number proposed by Wei et al. (1998). The solids dispersion coefficient (C_v) was calculated using Eq. (1), where $\tilde{\sigma}_{sd}$ is the standard deviation of the solid volume fraction and $\overline{x}$ is the mean value of the property in the points of the cross section. The radial Péclet number (Pe_{sr}) is given by Eq. (2), where f_s is the mean solid volume fraction at the points and the Reynolds number is calculated using the solid velocity, a particle density of 2450 kg/m^3 and a viscosity of 1.7×10^{-5} PaS.

$$C_v = \frac{\tilde{\sigma}_{sd}}{\overline{x}} \tag{1}$$

$$Pe_{sr} = 225.7(1 - f_s)^{-0.29} Re^{0.43} \tag{2}$$

13.3 Results and Discussion

13.3.1 Solid Velocity

Figure 3 presents a comparison of the solid velocity profiles for the gas-solid flow in the riser with ring baffles, with ultrasonic waves, and without these two methods. The solid velocity profiles presented in Fig. 3a–d are situated in the symmetrical axis of the riser, while the solid velocity profiles illustrated in Fig. 3e–h are situated in the unsymmetrical axis of the riser which is parallel to the solids inlet. These are the transversal lines that go from one wall to the other, passing through $r = 0$. In the unsymmetrical axis, the solid velocity profiles of the three cases are similar and have a minor deviation from the expected axisymmetric profile on the left side, because of the larger solids concentration in these regions. With ring baffles, this deviation is slighter and the velocity profiles are closed to an axisymmetric behavior. Also, solid velocity increases in some regions of the ring-baffled riser concerning the standard case. In the operating conditions C1 and C2, the solids velocity slightly decreases using ultrasound, but if the fluctuations are considered, the velocity profiles are substantially the same. However, the cross-flow generated by the ultrasonic waves regarding the ascendant gas-solid flow produces a contrary effect to the desired one on its dispersion. It can be checked especially in conditions C1 and C2, where the gas velocity of the ascendant flow is smaller. Otherwise, an increase in the solid velocity can be noted near one of the walls of the ring-baffled riser in Fig. 3b, f because of the reduction of the opening area in the region of the rings. In the operating condition C3, the solid velocity increased with respect to the standard case in one of the walls, both with ultrasound and ring baffles. However, the solid velocity profile on the unsymmetrical axis became smoother with ultrasound (Fig. 3g). In the operating condition C4, only the ring baffles changed the solid velocity with respect to the standard case.

The solid velocity was modified in the unsymmetrical axis (Fig. 3e–h) with respect to the standard case using ring baffles and acoustic waves, but not in all the cases. In the operating condition C1, there was no velocity variation in the case with ultrasound relative to the standard case. With ring baffles, the velocity variation was greater on the wall parallel to the solids inlet. However, the velocity increased on the wall opposite to that, where more particles accumulate. In the operating condition C2, there was a decrease in the solid velocity with the use of ring baffles on the wall opposite the solids inlet and an increase in velocity on the other wall. In this operating condition, the solid velocity was not modified with the use of ultrasound; however, its behavior Is similar in both cases—ring baffles and ultrasound—on the wall opposite to the solids inlet. In the operating conditions C3 and C4, the solid velocity profiles are more symmetric because the gas superficial velocity is higher than in the other conditions It causes a more diluted flow and reduces the thickness of the core-annulus profile. The solid velocity profile in condition C3 (Fig. 3g) is more unsymmetrical with ring baffles and a decrease of these values near the wall is observed near the wall. With the use of ultrasound, there is a slight increase in the solid velocity in the same region

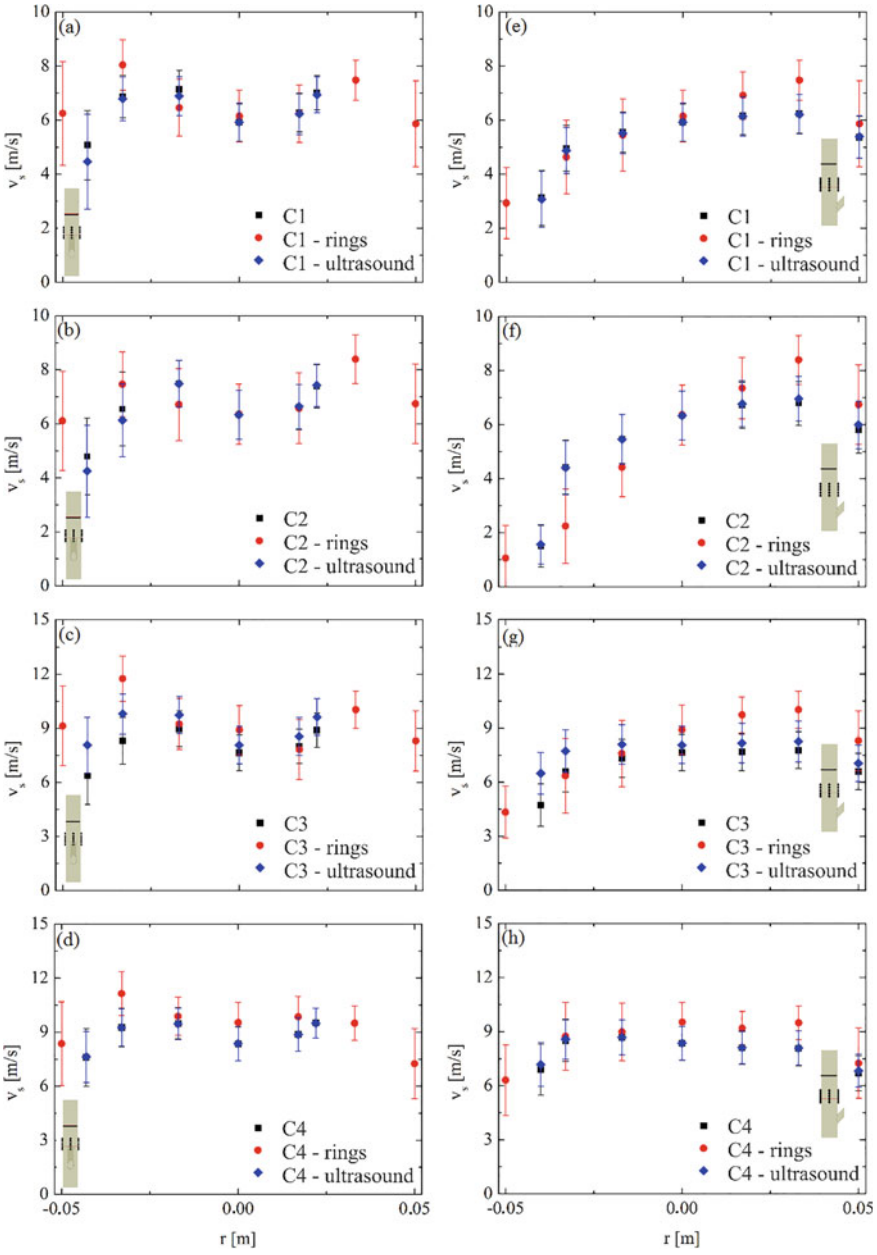

Fig. 3 Solid velocity profiles of the four operating conditions with and without ring baffles and with the influence of the acoustic field. The error bars are the RMS values of the variables

regarding the standard case and uniform distribution of velocities along the axis. In condition C4, the velocity profiles were not modified considering the fluctuation values.

The RMS values in Fig. 3 show the mean solid velocity fluctuation during the acquisition time of the PDA measurements. In the symmetrical axis of the riser, both the ring baffles and the ultrasonic waves increase solid velocity fluctuation near the wall. Otherwise, lower solid velocity fluctuation is observed in the unsymmetrical axis with the use of ultrasonic waves. The lower values of velocity fluctuation are observed near the wall opposite to the solids inlet, where the solids concentration is higher. It suggests that the particle clusters were not broken but increased, as shown in the next results. However, in the operating condition C2, even though particle clusters were not broken, solid velocity became negative near the wall considering the RMS values in the unsymmetrical axis, with the use of ring baffles. At least 10,000 values of solid axial velocity were gathered with PDA at each point, with an error lower than 1%. The raw data showed a normal distribution and some negative values of velocity were observed, which was associated with the fall of particles that, consequently, lead to back mixing.

13.3.2 Solid Volume Fraction

In Fig. 4, the solid volume fraction contours of the three cases are compared at 0.80 m above the base of the riser, calculated using the solids concentration and the average Sauter diameter given by the PDA technique at each measurement point. The standard cases in the four operating conditions (C1, C2, C3, and C4) are in the first line, followed by the cases with ring baffles and with ultrasound. In the operating conditions C1 and C2, the ring baffles contribute to a better solids dispersion, decreasing its concentration in the annular region and improving the distribution of solids along the cross section. In these cases, the use of ultrasound increased the concentration of particles in the annular region and reduced dispersion. In the operating conditions, C3 and C4 both ring baffles and ultrasound contributed to promoting the solids dispersion. In the cases with ring baffles, the particles are redirected to the center of the riser and accumulate in this region. With acoustic waves, there is a slight accumulation of particles in the center and their dispersion along the cross section is similar to that observed with ring baffles. Regarding the core-annulus profile, the ring baffles contributed to breaking it in the measured position. Ultrasound was not able to reduce the concentration of solids near the wall under operating conditions C1 and C2, in which the fast fluidization regime is dominant. One reason for this result may be that the superficial velocity of the flow is low relative to the solids mass loading, causing the pressure drop to be greater and there is a back mixing. Also, it can be noted a large difference in the solid volume fraction distributions in Fig. 4, although the difference in velocity profiles between the 3 cases (standard, ring baffles, and ultrasound) is minimum. The velocity component measured with the PDA technique is the axial component. With ultrasound, the greatest change in velocity takes place

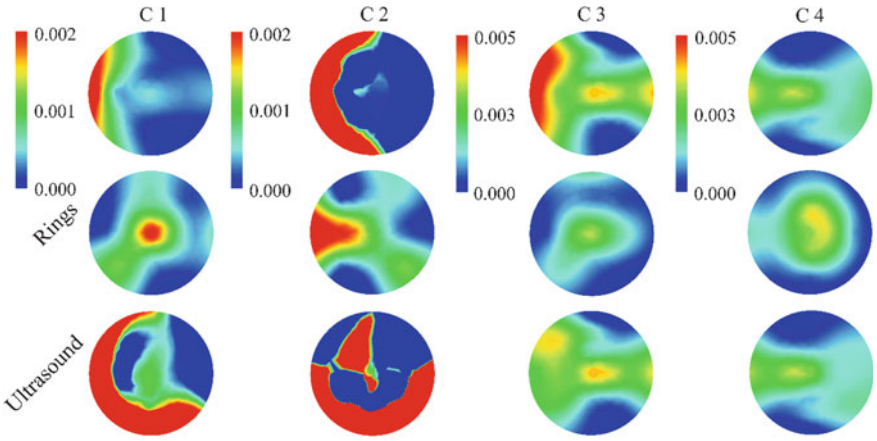

Fig. 4 Solid volume fraction contours in the riser cross section at 0.80 m height in the operating conditions C1, C2, C3, and C4 with and without ring baffles and with the influence of ultrasonic waves

in the radial direction, which is the direction of propagation of the emitted acoustic waves. This difference in the radial velocity causes the significant change observed in the distribution of solid particles in the cross section. Similar behavior can be attributed to the flow with ring baffles since they redirect the particles near the wall toward the center of the riser. In the ring-baffled riser, however, the axial velocity increases in some points because the opening area of the flow decreases near the baffles.

13.3.3 Gas-Solid Dispersion

The gas-solid dispersion was evaluated using the radial Péclet number, which is the product between the Reynolds number and the Schmidt number of the solids flow. The Péclet number is the product between the Reynolds number and the Schmidt number of the gas-solid flow and relates the importance of convective and diffusive effects on the gas-solid dispersion. It is common to use the modified Péclet number to assess the gas-solid dispersion in CFB risers (Breault 2006), as this parameter considers not only the volume fraction but also the velocity of the solid particles, resulting in a more complete analysis than if only the solid volume fraction was considered. Figure 5 shows the contours of these variables in the cross section at a height of 0.80 m. In the first line are the standard cases (C1, C2, C3, and C4) in the four operating conditions studied. The same operating conditions with the use of ring baffles and ultrasonic waves to disperse solid particles are illustrated in the second and third lines. In the operating condition C1, the radial Péclet number increased on the wall with the use of rings, however, the distribution of this variable in the

cross section is more homogeneous in the standard case and with ultrasound. In the operating condition C2, both rings and ultrasound increased the Péclet number near to the riser wall. With rings, there are higher Pe_{sr} values on the walls and smaller ones in the center. With ultrasound, the distribution of particles in the center of the riser was not modified and there was an increase in Pe_{sr} in the wall region. In the operating conditions C3 and C4, there was little influence of ultrasound on the Péclet number, but a better distribution is noted in case C3 with ultrasound, in which there an increase in Pe_{sr} was observed in the wall region. With rings, there is an increase in Pe_{sr} values close to the wall and a slight decrease in the center of the duct in the operating condition C3. The lower influence of ultrasound on the gas-solid dispersion in condition C4 is because this condition has a dilute homogeneous flow, with dispersion that is satisfactory even without the use of dispersion techniques. In conditions C1 and C2, which are of fast fluidization regime, there is a higher solids loading and a tendency to develop clusters due to the number of collisions between particles. Visually, the performance of the ultrasound in increasing the gas-solid dispersion was better in the operating condition C3, in which solids concentration and superficial velocity are higher compared to the other conditions. It provides more dispersion of the acoustic energy by the particles and less impact on the pressure drop compared to conditions C1 and C2.

Using ring baffles improves the gas-solid dispersion near the wall because there is an increase in solids velocity in this region that is attributed to the decrease in the opening area. Also, the solid particles are redirected from the wall to the center of the riser, and their momentum increase in the radial direction. When the increase in Pe_{sr} is very large on the walls, its value decreases in the center of the riser, which is

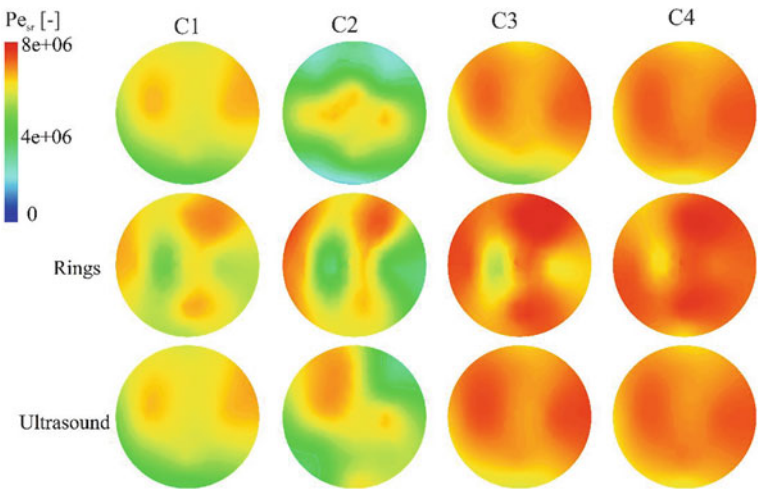

Fig. 5 Radial Péclet number (Pe_{sr}) of the four operating conditions with and without ring baffles and under the influence of the acoustic field at 0.80 m height

not desirable. To avoid this behavior, a large increase in the superficial velocity must be avoided, as this can cause the bed dilution and lower gas-solid dispersion.

To quantify the solids dispersion in the cross section of the riser, the solids dispersion coefficient and the radial Péclet were calculated for the cross section in each case, at 0.80 m above the base of the riser, as shown in Fig. 6. In the operating condition C1, the dispersion coefficient decreased by 51% with rings and increased by 60% with ultrasound. In condition C2, there was a decrease of 72% with rings and 24% with ultrasound. In conditions C3 and C4 there was a decrease in the dispersion coefficient in both cases. With rings, the decrease was 5% and 8% with ultrasound. In condition C4, it was 16% with rings and 10% with ultrasound. In the analysis of the radial Péclet number, an increase in the value of the variable compared to the standard case shows that the gas-solid dispersion improved. The greatest Péclet number values were observed in case C2 with acoustic waves and in case C3 with rings. In the operating condition C3, both techniques improve the dispersion of particles, but the rings provide a better result. In operating condition C2, the gas-solid dispersion improves a lot with the use of ultrasound and worsens with the use of ring baffles. This result differs from the analysis of the dispersion coefficient, which shows that the solids dispersion with the use of rings improves in condition C2. It is noteworthy that the Péclet number provides more complete results of the gas-solid dispersion, as it considers the solid velocity and the solid volume fraction. The statistical dispersion coefficient considers only the mean solid volume fraction and its standard deviation in the cross section. In the operating condition C1, it is also noted that the statistical dispersion coefficient shows lower solids dispersion with ultrasound, which is not observed considering the Péclet number. In the operating condition C4, the dispersion coefficient shows that the dispersion worsens with both techniques, but there is an increase in the Péclet number with the use of ring baffles. The best gas-solid dispersion with ultrasound was obtained in the cases where the solids loading is higher and, thus, the acoustic field interacts with a larger number of particles. With the use of ring baffles, the best gas-solid dispersion considering the Péclet number was obtained with the highest solids velocity, equal to 8.3 m/s.

13.4 Conclusions

Considering these results, both dispersion techniques presented are feasible to increase the contact between the solid particles and the gas phase in a CFB riser. Although ultrasound cannot break the core-annulus profile under the conditions of rapid fluidization analyzed, its use increases the gas-solid contact in the radial direction, as verified through the Péclet number. However, it is necessary to test the effect of acoustic waves on the flow under other operating conditions, by applying different sound frequencies and electrical powers in the transducers. Ring baffles are an intrusive way to reduce the core-annulus profile development in the flow and to break particle clusters. Using ring baffles in extended operating campaigns leads to wear and erosion, and that must be analyzed together with the pressure drop generated

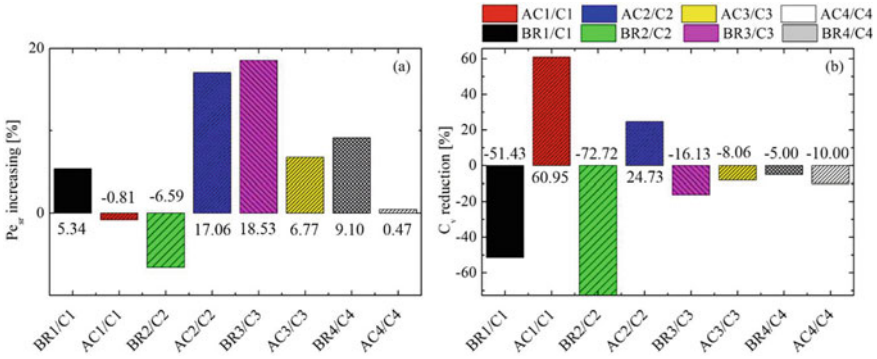

Fig. 6 Increasing in the radial Péclet number (Pe_{sr}) and reduction in the solids dispersion coefficient (C_v) with acoustic waves and ring baffles in comparison with the standard measurements in the four operating conditions (C1, C2, C3, C4). BR refers to the cases with ring baffles and AC, to the cases with ultrasonic waves

because of the reduction of the opening area. Also, it is necessary to assess, for both techniques, in which axial positions new deflectors or transducer sets should be positioned to prevent the core-annulus profile to develop again and reducing the gas-solid contact.

Acknowledgements The authors are grateful for the financial support of this research from Petróleo Brasileiro S.A. (Petrobras), through the cooperation agreements 0050.0070 334.11.9 and 5850.0103010.16.9, and from the National Council for Scientific and Technological Development (CNPq), under process number 308714/2016-4. This study was financed in part by the Coordenação de Aperfeiçoamento de Pessoal de Nível Superior - Brasil (CAPES).

References

Bi HT, Grace JR (1995) Flow regime diagrams for gas-solid fluidization and upward transport. Int J Multiph Flow

Breault RW (2006) A review of gas-solid dispersion and mass transfer coefficient correlations in circulating fluidized beds. Powder Technol

Da Rosa LM, Bastos JCSC, Mori M, Martignoni WP (2008) Simulation of a high-flux riser-reactor flow using CFD techniques. AIChE Annu Meet Conf Proc

Ferschneider G, Mège P (2002) Dilute gas-solid flow in a riser. Chem Eng J 87(1):41–48

Gan J, Yang C, Li C, Zhao H, Liu Y, Luo X (2011) Gas–solid flow patterns in a novel multi-regime riser. Chem Eng J 178:297–305

Helland E, Bournot H, Occelli R, Tadrist L (2007) Drag reduction and cluster formation in a circulating fluidised bed. Chem Eng Sci

Jiang P, Bi H, Jean RH, Fan LS (1991) Baffle effects on performance of catalytic circulating fluidized bed reactor. AIChE J 37(9):1392–1400

Marzo A, Barnes A, Drinkwater BW (2017) TinyLev: a multi-emitter single-axis acoustic levitator. Rev Sci Instrum 88(8)

Namkung W, Kim SD (1998) Gas backmixing in a circulating fluidized bed. Powder Technol

Rossbach V, Padoin N, Meier HF, Soares C (2020) Influence of acoustic waves on the solids dispersion in a gas-solid CFB riser: numerical analysis. Powder Technol 359:292–304

Rossbach V, Utzig J, Decker RK, Meier HF (2016a) Experimental analysis of the gas-solid flow in a ring-baffled CFB riser using Laser Doppler Anemometry (LDA) and Phase-Doppler Anemometry (PDA). In: Proceedings of EPTT 2016a—10th ABCM spring sch transit turbul

Rossbach V, Utzig J, Decker RK, Noriler D, Meier HF (2016b) Numerical gas-solid flow analysis of ring-baffled risers. Powder Technol

Rossbach V, Utzig J, Decker RK, Noriler D, Soares C, Meier HF (2019) Gas-solid flow in a ring-baffled CFB riser: numerical and experimental analysis. Powder Technol 345

Wei F, Cheng Y, Jin Y, Yu Z (1998) Axial and lateral dispersion of fine particles in a binary-solid riser. Can J Chem Eng

Yan WC, Li J, Luo ZH (2012) A CFD-PBM coupled model with polymerization kinetics for multizone circulating polymerization reactors. Powder Technol 231:77–87

Werther J (1999) Measurement techniques in fluidized beds. Powder Technol 102:15–36

Zhou W, Zhao C, Duan L, Liu D, Chen X (2011) CFD modeling of oxy-coal combustion in circulating fluidized bed. Int J Greenh Gas Control 5:1489–1497